

## How well do integrated 3D models predict alveolar defects after treatment with clear aligners?

Ting Jiang<sup>a</sup>; Jian Kai Wang<sup>a</sup>; Yang Yang Jiang<sup>b</sup>; Zheng Hu<sup>b</sup>; Guo Hua Tang<sup>c</sup>

### ABSTRACT

**Objectives:** To evaluate the accuracy of integrated models (IMs) constructed by pretreatment cone-beam computed tomography (pre-CBCT) in diagnosing alveolar defects after treatment with clear aligners.

**Materials and Methods:** Pre-CBCT and posttreatment cone-beam computed tomography (CBCT) scans from 69 patients who completed nonextraction treatment with clear aligners were collected. The IMs comprised anterior teeth in predicted positions and alveolar bone from pre-CBCT scans. The accuracy of the IMs for identifying dehiscences or fenestrations was evaluated by comparing the means of the defect volumes, absolute mean differences, and Pearson correlation coefficients with those measured from post-CBCT scans. Defect prediction accuracy was assessed by sensitivity, specificity, positive predictive values, and negative predictive values. Factors possibly affecting changes in mandibular alveolar defects were analyzed using a mixed linear model.

**Results:** The IM measurements showed mean deviations of  $2.82 \pm 9.99 \text{ mm}^3$  for fenestrations and  $3.67 \pm 9.93 \text{ mm}^3$  for dehiscences. The absolute mean differences were  $4.50 \pm 9.35 \text{ mm}^3$  for fenestrations and  $5.17 \pm 9.24 \text{ mm}^3$  for dehiscences. The specificities of the IMs were higher than 0.8, whereas the sensitivities were both lower (fenestration = 0.41; dehiscence = 0.53). The positive predictive values were unacceptable (fenestration = 0.52; dehiscence = 0.62), and the overall reliability was low (<0.80). Molar distalization and proclination were positively correlated with significant increases in alveolar defects at the mandibular incisors after treatment.

**Conclusions:** Alveolar defects after clear aligner treatment cannot be simulated accurately by IMs constructed from pre-CBCT. Caution should be taken in the treatment of crowding with proclination and molar distalization for the safety of alveolar bone at the mandibular incisors. (*Angle Orthod*. 2020;91:313–319.)

**KEY WORDS:** Clear aligners; Alveolar defects; CBCT; Integrated model

<sup>a</sup> Resident Doctor, Department of Orthodontics, Shanghai Ninth People's Hospital, College of Stomatology, Shanghai Jiao Tong University School of Medicine, Shanghai, China.

<sup>b</sup> Orthodontist, Department of Orthodontics, Shanghai Ninth People's Hospital, College of Stomatology, Shanghai Jiao Tong University School of Medicine, Shanghai, China.

<sup>c</sup> Professor, Department of Orthodontics, Shanghai Ninth People's Hospital, College of Stomatology, Shanghai Jiao Tong University School of Medicine; and National Clinical Research Center for Oral Diseases, Shanghai Key Laboratory of Stomatology & Shanghai Research Institute of Stomatology, Shanghai, China.

Corresponding author: Dr Guo Hua Tang, Department of Orthodontics, Shanghai Ninth People's Hospital, College of Stomatology, Shanghai Jiao Tong University School of Medicine, #639 ZhiZaoJu Rd., Shanghai 200011, China (e-mail: drtanggh@163.com)

Accepted: November 2020. Submitted: April 2020.

Published Online: January 25, 2021

© 2021 by The EH Angle Education and Research Foundation, Inc.

### INTRODUCTION

Alveolar bone defects are anatomical variations between the teeth and alveolar bone. A V-shaped defect resulting in lowering of the crestal bone margin to expose the root surface is defined as an alveolar dehiscence.<sup>1</sup> When there is still some bone in the cervical region, the defect is a fenestration.<sup>2</sup> Previous studies showed that alveolar defects were highly prevalent in patients with malocclusions, which increases the difficulty and complexity of orthodontic treatment.<sup>3,4</sup> Since orthodontic treatment is based on the biological events of bone resorption and bone remodeling that occur in the direction of tooth movement, alveolar defects might be created or exacerbated during treatment.

Orthodontic tooth movement through an atrophic alveolar ridge increased bone dehiscence in the buccal plate.<sup>5</sup> Nonextraction treatment for crowding was also

associated with greater buccal bone loss in the anterior tooth area, even when using clear aligners, which are usually thought to have superior periodontal health compared with fixed appliances.<sup>6,7</sup> In particular, the mandibular anterior region had a higher risk of bone loss, possibly due to the thin buccal alveolar bone thickness of 0.2–0.6 mm on average.<sup>8</sup> Significant loss of bony support is detrimental to the periodontium and negatively affects the long-term health of the teeth.

To avoid these side effects, some digital systems fabricating customized orthodontic appliances have been proposed that use an integrated three-dimensional (3D) model with root and jaw information created from a pretreatment cone-beam computed tomography (pre-CBCT) image to help predict alveolar defects after treatment, which would allow for safer treatment planning with limited patient radiation exposure.<sup>9,10</sup> However, the reliability of this approach has not been demonstrated previously. Consequently, this study aimed to use a clear aligner system as an example to assess the accuracy of integrated 3D models for predicting alveolar defects after treatment and to analyze possible factors that affected changes in the volume of mandibular anterior alveolar defects.

## MATERIALS AND METHODS

### Patient Selection

Patients treated with Invisalign (Align Technology, Santa Clara, Calif) between January 2016 and December 2018 were selected.

### Inclusion Criteria

The following inclusion criteria were used:

- Age  $\geq 20$  years;
- Crowding that could be resolved using molar distalization and/or proclination and/or expansion and/or interproximal enamel reduction;
- Completion of all active stages of treatment with the first series of aligners;
- Availability of cone-beam computed tomography (CBCT) scans before and after treatment;
- No auxiliary device, such as segmental wires, used on the incisors;
- Voxel size for CBCT ranging from 0.20 mm to 0.30 mm.

### Exclusion Criteria

The following exclusion criteria were used:

- Unclear CBCT images of the teeth and jaws;
- Presence of an alveolar cleft or other bone defects;
- Bite jumping designed in the virtual setup.

Both pre-CBCT and posttreatment CBCT (post-CBCT) scans were collected and evaluated. Institutional ethical review board approval was obtained to conduct this study, and the data use was approved by the ethics committee of Shanghai Ninth People's Hospital (SH9H-2018-T63-1).

### Volume of Alveolar Bone Defects Measured from CBCT Scans (Direct Method)

The CBCT files were imported into Mimics 19.0 (Materialise, Leuven, Belgium). The buccolingual and mesiodistal axes of each anterior tooth were adjusted to show the total length of each root in cross-sectional and axial slices. In the sagittal plane, the cross-sectional axis placed on the higher point of the labial or lingual alveolar crest represented the original crestal margin. Images that showed that the root was surrounded by no cortical bone in at least three successive views were registered as having an alveolar defect (Figure 1, A1–A4).<sup>3</sup> This lack of bone was classified as dehiscence when the alveolar bone defects involved the alveolar crest and as fenestration when the defects did not.

The cortical discontinuity points were marked on each cross-sectional slice (Figure 1, B1), and the region of root exposure representing the alveolar defect was outlined manually, which ensured detailed slice-by-slice segmentation of the defect borders (Figure 1, B2). The defects were reconstructed into 3D volumes from the areas outlined on each slice of the known thickness and then imported into Magics 21.0 (Materialise) to calculate the total volume (Figure 1, C1 and C2).

The volumes of the defects in anterior teeth measured directly from pre-CBCT scans were recorded as V0, and the post-CBCT measurements were recorded as V1.

### Volume of Alveolar Defects Predicted by Integrated Models (Indirect Method)

The pre-CBCT files were imported into Mimics software, and threshold segmentation of all three views (sagittal, coronal, and transverse) was performed individually on the data to generate separate 3D models of the maxilla and mandible. The same process was performed to create 3D models of each individual anterior tooth.

The pretreatment dentition (pre-D) and virtual dentition (vir-D) from ClinCheck (Align Technology) were imported into 3-matic software, version 19.0 (Materialise). Automated registration based on the characteristic surface of the pre-D and pretreatment jaws (from pre-CBCT) was performed using the crowns as areas of optimal overlap after an initial registration. The 3D

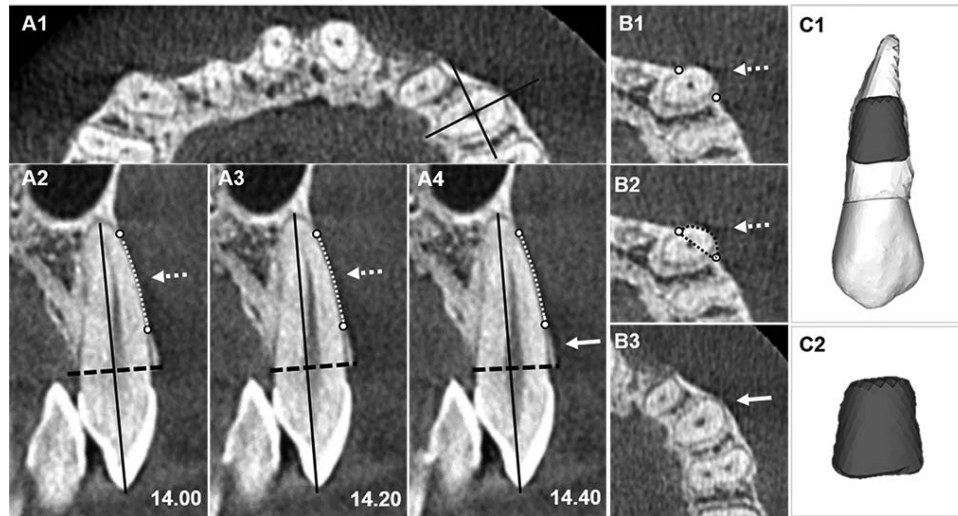


**Figure 1.** Volumetric measurement of alveolar bone defects (fenestration) from CBCT scans. Axes (solid line) of the maxillary canine were adjusted to show the total length of the root in cross-sectional (A1) and axial (A2) slices. The cross-sectional axis (dashed black line) placed on the higher point of the labial or lingual alveolar crest represents the original crestal margin (A2–A4). Images showing that the root was surrounded by no cortical bone in at least 3 successive views were registered as having an alveolar defect (A2–A4, dashed white line). The cortical discontinuity points were marked on a cross-sectional slice (B1), and the region of root exposure was outlined (B2, dashed line). Continuous cortical bone is shown in B3. Slice by slice, the defects were reconstructed into 3D volumes (C1) and imported into Magics 21.0 to calculate the total volume (C2).

positions of the roots were generated by superimposing the crown of each individually segmented CBCT tooth onto the corresponding crown of the vir-D. Since the pre-D and vir-D were in a shared coordinate system, the final integrated 3D model was thus reconstructed by the predicted crowns from vir-D with the matched roots and the jaws with alveolar bone from pre-CBCT (Figure 2). The integrated model (IM) was then imported into Magics software, and the Boolean operation (subtraction) was performed on pretreatment jaws and roots to calculate the amount of root exposure, which was recorded as the volume of alveolar defects predicted by the integrated models.

Intra- and interinvestigator measurement agreement of the alveolar defect volume was assessed by calculating intraclass correlation coefficients. Sixty teeth were randomly sampled from all CBCT scans. Two investigators measured the volume of defects independently to evaluate interinvestigator agreement. One of the investigators then repeated these measurements 2 weeks later to assess intrainvestigator agreement.

**Statistical Analysis**

Statistical comparisons were carried out using Wilcoxon tests to examine differences between V0 and V1. Differences in the incidence of bone defects were examined by  $\chi^2$  tests, and the significance level was set at  $P = .050$ . The accuracy of IMs (indirect method) was assessed by comparing the means and

absolute mean differences with the measurements from post-CBCT (direct method). The relationship between the two methods was estimated using Pearson correlation coefficients. Specificity, sensitivity, and positive and negative predictive values were calculated for the indirect method. These statistical analyses were performed using SAS 8.02 software (SAS Institute, Cary, NC). Possible impacts of different types of malocclusion and treatment modalities on changes in the volumes of mandibular anterior alveolar defects were analyzed using a mixed linear model in Eviews 6.0 (Quantitative Micro Software, Irvine, Calif).

**RESULTS**

From 69 patients (44 women, 25 men; age range = 20–41 years; mean age =  $28.50 \pm 5.67$  years), a total of 828 teeth were evaluated and measured. The distribution of malocclusions and treatment modalities is shown in Table 1. The intraclass correlation coefficients for inter- and intrainvestigator measurement agreement were 0.92 (95% confidence interval = 0.86 to 0.95) and 0.94 (95% confidence interval = 0.89 to 0.96), respectively.

Only one mandibular central incisor had a fenestration of  $3.20 \text{ mm}^3$  on the lingual side before treatment. After treatment, defects on the lingual side were not detected by CBCT or predicted by the IMs. Given this situation, only labial defects are presented in the results.

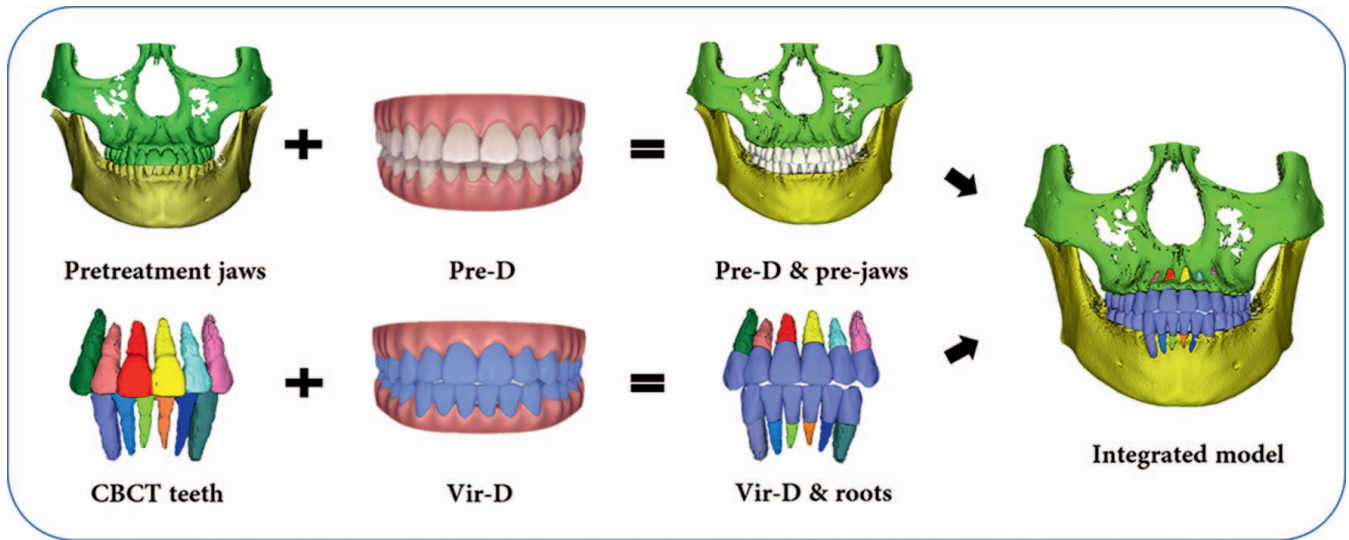


**Figure 2.** Reconstruction of the IM. The models of pretreatment jaws were reconstructed from pretreatment CBCT scans. Surface characteristic-based automated registration of the pretreatment dentition model (pre-D) and the pretreatment jaws was performed using the crowns as areas of optimal overlap. CBCT teeth were superimposed individually onto the corresponding crowns of the virtual setup (vir-D). Due to the pre-D and vir-D being on the same coordinate system, the vir-D and roots were superimposed on the pretreatment jaws, and the final integrated model was finished.

**Differences in Alveolar Defects Between V0 and V1**

Of 828 teeth evaluated, 446 (53.86%) had alveolar defects before treatment, and 236 (52.91%) appeared in the maxilla. In the maxilla, fenestrations were seen with greater frequency (81.78%), whereas in the mandible, dehiscences were more common (80.95%). After treatment, 489 teeth (59.06%) had alveolar defects (from post-CBCT), which was significantly more than before treatment ( $P = .033$ ). The incidence of dehiscence in the lower incisors was significantly higher than before treatment (Table 2).

The average volume of alveolar defects per tooth (calculated only for those who had alveolar defects either before treatment and/or after treatment) was  $18.47 \pm 19.80 \text{ mm}^3$  before treatment, which was not significantly different from the volume measured with post-CBCT ( $16.79 \pm 14.09 \text{ mm}^3$ ;  $P = .809$ ). However, the average volume of dehiscences at the mandibular incisors was significantly increased (Table 3).

No association between the severity of malocclusion (crowding or overjet) and changes in alveolar defects was detected by the mixed linear model. However, molar distalization, proclination, and interproximal enamel reduction had significant impacts on the

increase in bone defects at the mandibular incisors. The variation was positively correlated with molar distalization and proclination and negatively correlated with interproximal enamel reduction. For the lower canines, molar distalization and expansion had positive correlations (Table 4).

**Accuracy of IMs in Predicting Alveolar Defects**

The sensitivity, specificity, positive predictive values, and negative predictive values of the IMs for fenestrations and dehiscences are shown in Table 5. Mean values of bone defects per tooth measured from post-CBCT and IMs are shown in Table 6. The mean differences between each IM and post-CBCT measurements were  $2.82 \pm 9.99 \text{ mm}^3$  for fenestrations and  $3.67 \pm 9.93 \text{ mm}^3$  for dehiscences. The mean absolute difference was  $4.50 \pm 9.35 \text{ mm}^3$  for fenestrations and  $5.17 \pm 9.24 \text{ mm}^3$  for dehiscences. The correlations between post-CBCT and the IMs were relatively low ( $r < 0.80$ ) for all measurements.

**DISCUSSION**

Although the use of CBCT is not routine in orthodontics, it provides more diagnostic information.

**Table 1.** Distribution of Malocclusions and Treatments (No. of Cases)

Molar Relationship	Crowding	Overjet	Space-Gaining Measures
Class I (n = 41)	I° ( $\leq 4 \text{ mm}$ ) (n = 45)	I° (3 ~ 5 mm) (n = 44)	Molar distalization (n = 20)
Class II (n = 19)	II° (4 ~ 8 mm) (n = 24)	II° (5 ~ 8 mm) (n = 25)	Expansion (n = 28)
Class III (n = 9)	III° (>8 mm) (n = 0)	III° (> 8 mm) (n = 0)	Proclination (n = 27)
			Interproximal enamel reduction (n = 46)

**Table 2.** Incidence of Alveolar Bone Defects in Anterior Teeth Before (T0) and After (T1) Treatment<sup>a</sup>

Tooth Type (n)	Fenestration				Dehiscence			
	T0		T1		T0		T1	
	Max, %	Man, %	Max, %	Man, %	Max, %	Man, %	Max, %	Man, %
Central incisor (n = 276)	36.23	6.52	28.99	2.90	6.52	30.43	10.14	46.38*
Lateral incisor (n = 276)	31.88	8.70	39.86	3.62	11.59	37.68	15.94	52.17*
Canine (n = 276)	71.74	13.77	63.77	12.32	13.04	55.07	21.01	57.25

<sup>a</sup> Man indicates mandibular; Max, maxillary.  
 \* Significant difference between T0 and T1, *P* < 0.050.

**Table 3.** Volume (mm<sup>3</sup>) of Alveolar Bone Defects per Tooth Before (T0) and After (T1) Treatment (Mean ± SD)<sup>a</sup>

Tooth Type	Fenestration				Dehiscence			
	T0	n	T1	<i>P</i> Values	T0	n	T1	<i>P</i> Values
Max central incisor	13.26 ± 13.12	58	8.10 ± 7.65	.075	6.80 ± 6.56	15	18.27 ± 10.97	.665
Max lateral incisor	14.68 ± 15.72	60	14.67 ± 9.98	.713	8.63 ± 10.55	27	15.93 ± 10.84	.262
Max canine	38.04 ± 24.57	102	25.84 ± 17.17	.287	18.94 ± 24.43	31	17.71 ± 15.91	.746
Man central incisor	2.64 ± 2.16	11	1.82 ± 2.68	.420	5.80 ± 6.53	64	10.61 ± 7.32	<.001*
Man lateral incisor	3.64 ± 2.95	14	2.36 ± 4.62	.172	11.96 ± 11.08	74	18.55 ± 12.96	<.001*
Man canine	5.43 ± 4.48	23	17.09 ± 18.56	.003*	29.85 ± 15.97	82	20.52 ± 13.17	<.001*

<sup>a</sup> Only the tooth that had alveolar bone defect either before and/or after treatment was included in the table.  
 \* Significant difference between T0 and T1, *P* < .050.

**Table 4.** Factors Associated With Changes of Alveolar Bone Defects in Mandibular Anterior Teeth After the Treatment by Mixed Linear Model<sup>a</sup>

Factors	Man Incisors (n = 163)		Man Canines (n = 105)	
	Regression Coefficient	<i>P</i> Values	Regression Coefficient	<i>P</i> Values
Constant	4.15	.040*	-6.2517	.057
Crowding	0.40	.082	-0.3756	.077
Overjet	-0.26	.067	-0.7141	.061
Molar distalization	0.54	.049*	11.9489	.034*
Expansion	2.39	.081	7.8749	.011*
Proclination	1.58	.048*	6.1747	.062
Interproximal enamel reduction	-0.51	.034*	-3.3040	.048*

<sup>a</sup> Only the tooth that had alveolar bone defect either before or/and after the treatment was included in the table;  
 \* *P* < .050.

Assessing the integrity of periapical alveolar bone would help make a suitable treatment plan and contribute to the long-term stability of the outcome. Previous studies showed that CBCT scanning with voxel sizes of 0.20 to 0.30 mm, as selected in this study, had high measurement accuracy, and the direct method for measuring the volume of alveolar defects was reliable.<sup>11–13</sup> Multiple CBCT scans, however, must be weighed against the risk of increased radiation exposure compared with traditional radiographs.<sup>14</sup> Root and jaw information from pretreatment CBCT was thus suggested for integration into the virtual setup to avoid positioning the roots across the bony boundary. The present results, however, demonstrated that this approach was not accurate, at least for clear aligner therapy.

Compared with direct CBCT examination, IMs only predicted half of the defects, which might give clinicians a false sense of safety. Likewise, the positive

predictive values were low, which meant that most defects predicted by the IM did not truly develop (Table 5). One reason for this might be alveolar bone remodeling during orthodontic tooth movement. Instead of moving “in” the bone as simulated by the IM, the tooth may actually move “with” the bone. However, the extent of bone remodeling is limited, and the anatomic boundary does exist. Vardimon et al.<sup>15</sup> recommended using a 1:2 bone remodeling/tooth movement ratio as the guideline for determining the biocompatible range of tooth movements. It is important to note that the labial alveolar bone in the mandibular anterior area is always thin, and the dehiscence prevalence is higher in nature.<sup>16</sup> A change beyond 0.71 mm in the L1-NB distance by orthodontic treatment has been shown to correlate with extensive labial bone loss at the lower incisors.<sup>17</sup> Thus, treatment modalities such as expansion and proclination that tend to move teeth labially have higher risks for

**Table 5.** Sensitivity and Specificity of the Integrated Model for Detecting Alveolar Defects

Integrated Model	Fenestration	Dehiscence
Sensitivity	0.41	0.53
Specificity	0.88	0.83
Positive predictive value	0.52	0.62
Negative predictive value	0.81	0.78

alveolar defects, which was supported by previous studies and the current results (Table 4).<sup>17,18</sup>

According to the existing evidence, clear aligners are a viable alternative to conventional fixed orthodontic therapy in nonextraction treatment of mild to moderate malocclusions in nongrowing patients.<sup>19</sup> A similar study population was selected in the present study. In a more recent meta-analysis, however, clear aligner therapy showed less ideal treatment outcomes than fixed appliances.<sup>20</sup> Buschang et al.<sup>21</sup> pointed out that the setup in clear aligner software could not accurately reflect the final occlusion of the patients at the end of active treatment. This observation perhaps derives from the fact that clear aligners move the teeth mainly by tipping.<sup>22</sup> The accuracy of upper incisor torque on aligners was reported to be 42%, and the discrepancies between the planned and achieved root positions were nearly 2 mm.<sup>22,23</sup> The increase in fenestration but decrease in dehiscence in the mandibular canines after treatment, as shown in the present results, might result from lingual crown and buccal root tipping movement in the aligners (Table 3). Thus, in addition to bone remodeling, insufficient control of root movement with aligners might be another reason for the lower accuracy of IMs in predicting bone defects.

Since the accuracy and reliability of the IMs were low, and the results showed a significant reduction in bone volume on the labial side of the mandibular incisors after treatment (Table 3), alveolar defects

should be avoided at any cost during treatment. In addition to proclination, the mixed linear analysis revealed that molar distalization was another major factor associated with increases in mandibular alveolar defects (Table 4). Molar distalization is likely to result in labial movement of the incisors due to anchorage loss or the use of Class II elastics. Such tooth movement was not prescribed in the setup but was unavoidable during treatment. Interproximal enamel reduction, on the other hand, could reduce the need for excessive proclination or molar distalization, thus helping decrease the risk of alveolar defects.

This study assessed the accuracy of integrated models in clear aligner therapy. Other appliances with computer-assisted setups, such as customized labial or lingual fixed appliances, have been reported to have greater effectiveness in producing tooth positions prescribed by a virtual treatment plan.<sup>24,25</sup> Whether these fixed appliance systems could benefit from the prediction of root and bone relationships for treatment planning awaits further investigation. Additionally, factors such as tooth type and the direction and extent of root movement should be included in future studies.

## CONCLUSIONS

- Integrated 3D models did not predict alveolar defects accurately when treatment was performed using clear aligners.
- The posttreatment reduction of bone volume indicated that caution should be used during aligner therapy when relieving crowding with proclination, expansion, and molar distalization in the mandible.

## ACKNOWLEDGMENT

This work was supported by the Natural Science Foundation of Shanghai (19ZR1429600).

**Table 6.** Volume of Bone Defects (mm<sup>3</sup>) per Tooth Measured from Post-CBCT and Integrated Model (IM) and Measurement Accuracy by Mean Abs and Correlations<sup>a</sup>

Tooth Type (n)	Fenestration				Dehiscence			
	Mean ± SD (mm <sup>3</sup> )		Difference (Mean Abs ± SD)	Correlation	Mean ± SD (mm <sup>3</sup> )		Difference (Mean Abs ± SD)	Correlation
	Post-CBCT	IM			Post-CBCT	IM		
Max central incisor (n = 138)	3.41 ± 6.36	2.58 ± 5.48	3.73 ± 5.88	0.32	1.99 ± 6.70	0.64 ± 1.73	2.36 ± 6.46	0.10
Max lateral incisor (n = 138)	6.37 ± 9.80	3.98 ± 8.65	5.88 ± 8.60	0.40	3.12 ± 7.91	0.62 ± 1.47	3.36 ± 7.49	0.15
Max canine (n = 138)	19.10 ± 18.63	6.37 ± 13.86	14.07 ± 15.61	0.50	3.98 ± 10.51	1.58 ± 4.30	4.45 ± 9.79	0.21
Man central incisor (138)	0.14 ± 0.88	0.56 ± 1.42	0.65 ± 1.56	0.05	4.92 ± 7.27*	1.57 ± 2.57	4.34 ± 6.62	0.21
Man lateral incisor (n = 138)	0.24 ± 1.59	0.25 ± 0.91	0.36 ± 1.54	0.30	9.95 ± 13.26*	4.34 ± 8.44	7.14 ± 10.46	0.53
Man canine (n = 138)	2.85 ± 9.81	1.42 ± 6.11	2.33 ± 6.26	0.76	12.20 ± 14.31	5.36 ± 11.12	9.36 ± 11.60	0.48
Total (n = 828)	5.35 ± 11.79	2.53 ± 7.77	4.50 ± 9.35	0.54	6.02 ± 11.04	2.35 ± 6.38	5.17 ± 9.24	0.45

<sup>a</sup> IM indicates integrated model; Man, mandibular; Max, maxillary; mean Abs, mean of the absolute difference between each pair of IM and post-CBCT measurements; post-CBCT, posttreatment cone-beam computed tomography.

## REFERENCES

1. Watson WG. Expansion and fenestration or dehiscence. *Am J Orthod.* 1980;77:330–332.
2. Davies RM, Downer MC, Hull PS, Lennon MA. Alveolar defects in human skulls. *J Clin Periodontol.* 1974;1:107–111.
3. Evangelista K, Vasconcelos KF, Bumann A, Hirsch E, Nitka M, Silva MA. Dehiscence and fenestration in patients with Class I and Class II Division 1 malocclusion assessed with cone-beam computed tomography. *Am J Orthod Dentofacial Orthop.* 2010;138:133–135.
4. Yagci A, Veli I, Uysal T, Ucar FI, Ozer T, Enhos S. Dehiscence and fenestration in skeletal Class I, II, and III malocclusions assessed with cone-beam computed tomography. *Angle Orthod.* 2012;82:67–74.
5. Ramos AL, Santos MCD, Almeida MR, Mir CF. Bone dehiscence formation during orthodontic tooth movement through atrophic alveolar ridges. *Angle Orthod.* 2020;90:321–329.
6. Jäger F, Mah JK, Bumann A. Periodontal bone changes after orthodontic tooth movement with fixed appliances: a cone-beam computed tomographic study. *Angle Orthod.* 2017;87:672–680.
7. Hellak A, Schmidt N, Schauseil M, Stein S, Drechsler T, Korbmayer-Steiner HM. Influence of Invisalign treatment with interproximal enamel reduction (IER) on bone volume for adult crowding: a retrospective three-dimensional cone beam computed tomography study. *BMC Oral Health.* 2016;16:83–92.
8. Foosiri P, Mahatumarat K, Panmekiate S. Relationship between mandibular symphysis dimensions and mandibular anterior alveolar bone thickness as assessed with cone-beam computed tomography. *Dental Press J Orthod.* 2018;23:54–62.
9. Lee RJ, Weissheimer A, Pham J, Go L, de Menezes LM, Redmond WR. Three-dimensional monitoring of root movement during orthodontic treatment. *Am J Orthod Dentofacial Orthop.* 2015;147:132–142.
10. Lee RJ, Pham J, Choy M, et al. Monitoring of tyodont root movement via crown superimposition of single cone-beam computed tomography and consecutive intraoral scans. *Am J Orthod Dentofacial Orthop.* 2014;145:399–409.
11. Menezes CC, Janson G, da Silveira Massaro C, Cambiaghi L, Garib DG. Precision, reproducibility, and accuracy of bone crest level measurements of CBCT cross sections using different resolutions. *Angle Orthod.* 2016;86:535–542.
12. Esposito SA, Huybrechts B, Slagmolen P, et al. A novel method to estimate the volume of bone defects using cone-beam computed tomography: an in vitro study. *J Endod.* 2013;39:1111–1115.
13. Tayman MA, Kamburoğlu K, Küçük Ö, Ateş FS, Günhan MI. Comparison of linear and volumetric measurements obtained from periodontal defects by using cone beam-CT and micro-CT: an in vitro study. *Clin Oral Investig.* 2019;23:2235–2244.
14. Ting S, Attaia D, Johnson KB, et al. Can modifying shielding, field of view, and exposure settings make the effective dose of a cone-beam computed tomography comparable to traditional radiographs used for orthodontic diagnosis? *Angle Orthod.* 2020;90:655–664.
15. Vardimon AD, Oren E, Ben-Bassat Y. Cortical bone remodeling/tooth movement ratio during maxillary incisor retraction with tip versus torque movements. *Am J Orthod Dentofacial Orthop.* 1998;114:520–529.
16. Coşkun İ, Kaya B. Appraisal of the relationship between tooth inclination, dehiscence, fenestration, and sagittal skeletal pattern with cone beam computed tomography. *Angle Orthod.* 2019;89:544–551.
17. Matsumoto K, Sherrill-Mix S, Boucher N, Tanna N. A cone-beam computed tomographic evaluation of alveolar bone dimensional changes and the periodontal limits of mandibular incisor advancement in skeletal Class II patients. *Angle Orthod.* 2020;90:330–338.
18. Baysal A, Uysal T, Veli I, Ozer T, Karadede I, Hekimoglu S. Evaluation of alveolar bone loss following rapid maxillary expansion using cone-beam computed tomography. *Korean J Orthod.* 2013;43:83–95.
19. Papadimitriou A, Mousoulea S, Gkantidis N, Kloukos D. Clinical effectiveness of Invisalign® orthodontic treatment: a systematic review. *Prog Orthod.* 2018;19:37–60.
20. Papageorgiou SN, Koletsis D, Iliadi A, Peltomaki T, Eliades T. Treatment outcome with orthodontic aligners and fixed appliances: a systematic review with meta-analyses. *Eur J Orthod.* 2020;42:331–343.
21. Buschang PH, Ross M, Shaw SG, Crosby D, Campbell PM. Predicted and actual end-of-treatment occlusion produced with aligner therapy. *Angle Orthod.* 2015;85:723–727.
22. Zhang XJ, He L, Guo HM, Tian J, Bai YX, Li S. Integrated three-dimensional digital assessment of accuracy of anterior tooth movement using clear aligners. *Korean J Orthod.* 2015;45:275–281.
23. Simon M, Keilig L, Schwarze J, Jung BA, Bourauel C. Treatment outcome and efficacy of an aligner technique—regarding incisor torque, premolar derotation and molar distalization. *BMC Oral Health.* 2014;14:68.
24. Grauer D, Proffit WR. Accuracy in tooth positioning with a fully customized lingual orthodontic appliance. *Am J Orthod Dentofacial Orthop.* 2011;140:433–443.
25. Brent EL, Christopher JV, Thorsten G. Effectiveness of computer-assisted orthodontic treatment technology to achieve predicted outcomes. *Angle Orthod.* 2013;83:557–562.